Electronic Supplementary Material (ESI) for ChemComm.

Pillar[6]arene-based UV-responsive supra-amphiphile: synthesis, self-assembly, and application in dispersion of multiwalled carbon nanotubes in water

Jie Yang, Guocan Yu, Danyu Xia and Feihe Huang*

State Key Laboratory of Chemical Engineering, Department of Chemistry, Zhejiang University, Hangzhou 310027, P. R. China; Fax and Tel: +86-571-8795-3189; Email address: fhuang@zju.edu.cn.

Electronic Supplementary Information (18 pages)

1. Materials and methods

All reagents were commercially available and used as supplied without further purification. Solvents were either employed as purchased or dried according to procedures described in the literature. Compound **1** and water-soluble pillar[6]arene (**WP6**) were synthesized according to literature procedures.[S1] NMR spectra were collected on either a Bruker Avance DMX-400 spectrometer or a Bruker Avance DMX-500 spectrometer with internal standard TMS. UV-vis spectra were taken on a Shimadzu UV-2550 UV-vis spectrophotometer. The fluorescence experiments were conducted on a RF-5301 spectrofluorophotometer (Shimadzu Corporation, Japan). Transmission electron microscopy (TEM) investigation was carried out on a JEM-1200EX instrument. The critical aggregation concentration (CAC) values of **G** and **WP6⊃G** were determined on a DDS-307 instrument.

*2. Syntheses of compounds **G** and **DMPy***

Scheme S1. Synthetic route to **G**.

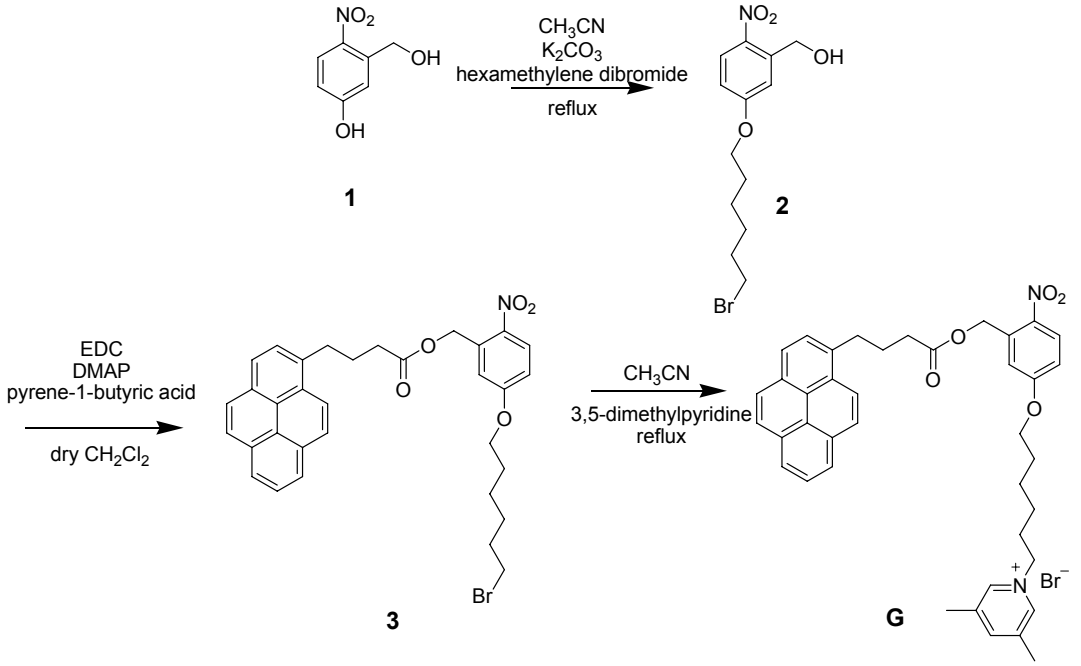

Synthesis of **2:** Hexamethylene dibromide (36.1 g, 148 mmol) and K_2CO_3 (9.95 g, 72.0 mmol) were added to a solution of 5-hydroxy-2-nitrobenzyl alcohol (2.50 g, 14.8 mmol) in CH_3CN (100 mL). The mixture was heated in a three-necked flask under nitrogen atmosphere at reflux for 24 h. The cooled reaction mixture was filtered and washed with chloroform. The filtrate was evaporated under vacuum, and the residue was further purified by flash column chromatography on silica gel (petroleum ether /ethyl acetate = 4:1, *v*/*v*) to afford **2** as a yellowish solid (2.52 g, 51%), m.p. 99.5–101.2 °C. The ^{1}H NMR spectrum of **2** is shown in Fig. S1. ^{1}H NMR (400 MHz, chloroform-*d*, 293 K) δ (ppm): 8.17 (d, J = 8 Hz, 1H), 7.20 (d, J = 4 Hz, 1H), 6.88 (d, J = 4 Hz, 1H), 4.98 (d, J = 4 Hz, 2H), 4.08 (t, J = 8 Hz, 2H), 3.43 (t, J = 8 Hz, 2H), 2.70 (t, J = 8 Hz, 1H), 1.86 (m, 4H). The ^{13}C NMR spectrum of **2** is shown in Fig. S2. ^{13}C NMR (100 MHz, chloroform-*d*, 293 K) δ (ppm): 171.40, 163.74, 140.81, 139.73, 127.81, 113.94, 113.24, 68.55, 62.49, 60.47, 33.77, 32.56, 28.76, 27.78, 25.10, 21.01, 14.13. LRESIMS is shown in Fig. S3: *m*/*z* 349.0 $[M + NH_4]^+$. HRESIMS: *m*/*z* calcd for $[M + NH_4]^+$ $C_{13}H_{22}N_2O_4Br$, 349.0763; found 349.0756; error –2 ppm.

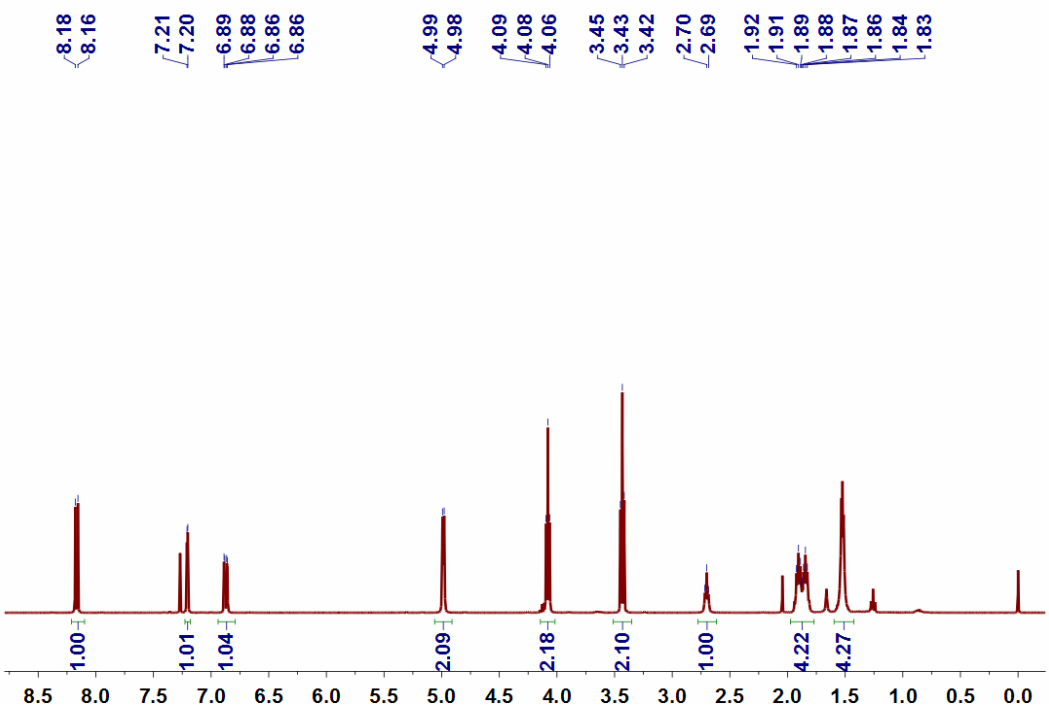

Fig. S1. ^{1}H NMR spectrum (400 MHz, chloroform-*d*, 293 K) of **2**.

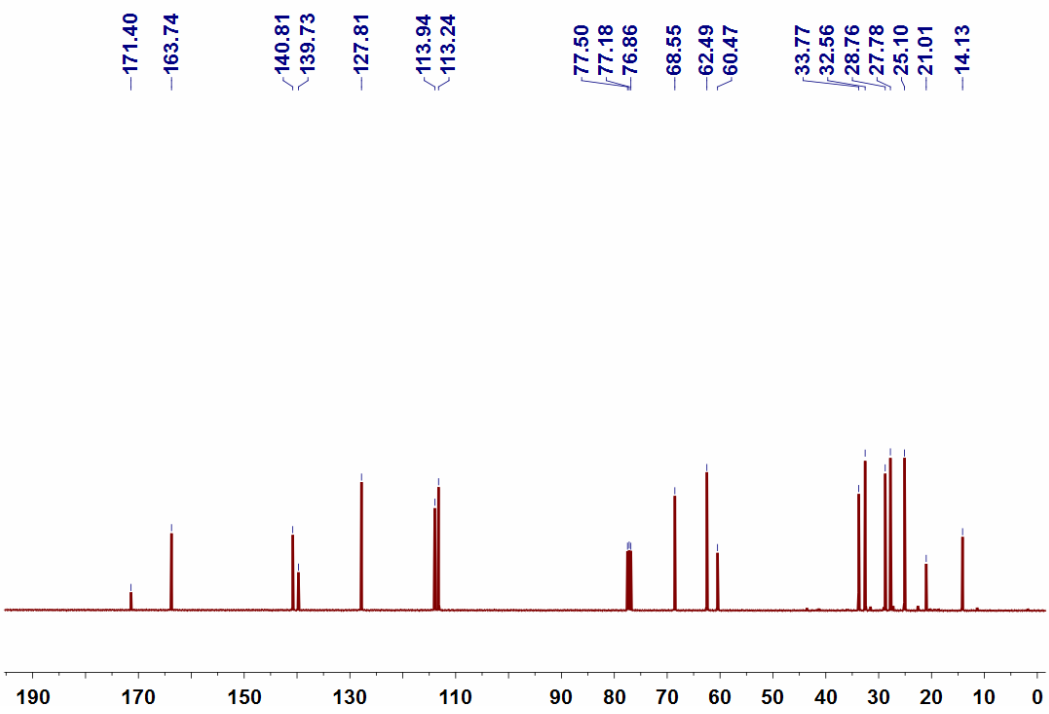

Fig. S2. ^{13}C NMR spectrum (100 MHz, chloroform-*d*, 293 K) of **2**.

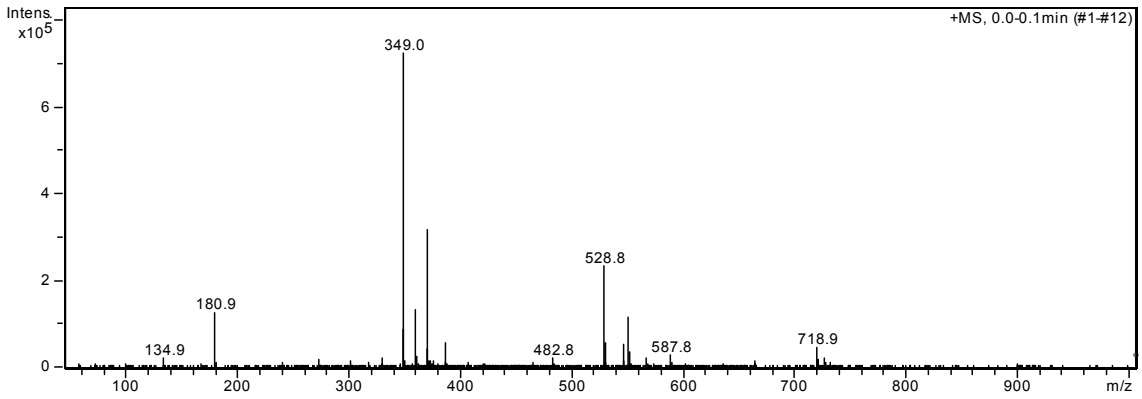

Fig. S3. Electrospray ionization mass spectrum of **2**. Assignment of the main peak: *m*/*z* 349.0 $[M + NH_4]^+$ (100%).

Synthesis of **3:** To a solution of **2** (1.15 g, 3.47 mmol) and pyrene-1-butyric acid (1.00 g, 3.47 mmol) in dry CH_2Cl_2 (50 mL), 4-dimethylaminopyridine (DMAP, catalytic amount) and 1-(3'-dimethylaminopropyl)-3-ethylcarbodiimide hydrochloride (EDC, 1.24 g, 6.94 mmol) were added under nitrogen atmosphere. The mixture was stirred overnight at room temperature. The solution was evaporated under vacuum and the residue was purified by flash column chromatography on silica gel (petroleum ether/ethyl acetate = 2:1, *v*/*v*) to afford **3** as a yellowish solid (1.28 g, 60%), m.p. 103.8−105.2 °C. The ^{1}H NMR spectrum of **3** is shown in Fig. S4. ^{1}H NMR (400 MHz, chloroform-*d*, 293 K) δ (ppm): 8.28 (d, J = 8 Hz, 1H), 8.14 (m, 3H), 8.09 (t, J = 8 Hz, 2H), 8.02 (s, 2H), 7.98 (t, J = 8 Hz, 1H), 7.86 (d, J = 8 Hz, 1H), 6.94 (d, J = 4 Hz, 1H), 6.80 (m, 1H), 5.51 (s, 2H), 3.89 (t, J = 6 Hz, 2H), 3.43 (t, J = 8 Hz, 2H), 3.34 (t, J = 6 Hz, 2H), 2.60 (t, J = 8Hz, 2H), 2.27 (t, J = 8Hz, 2H), 1.77 (t, J = 8Hz, 2H), 1.66 (t, J = 8 Hz, 2H), 1.36 (m, 4H). The ^{13}C NMR spectrum of **3** is shown in Fig. S5. ^{13}C NMR (100 MHz, chloroform-*d*, 293 K) δ (ppm): 172.69, 163.30, 140.00, 127.99, 125.08, 123.21, 114.08, 113.03, 68.49, 63.25, 33.85, 33.66, 32.73, 32.48, 30.93, 28.68, 27.72, 26.79, 25.07. LRESIMS is shown in Fig. S6: *m*/*z* 624.1 $[M + Na]^+$. HRESIMS: *m*/*z* calcd for $[M + NH_4]^+$ $C_{33}H_{36}O_5N_2Br$, 619.1808; found 619.1805; error –0.4 ppm.

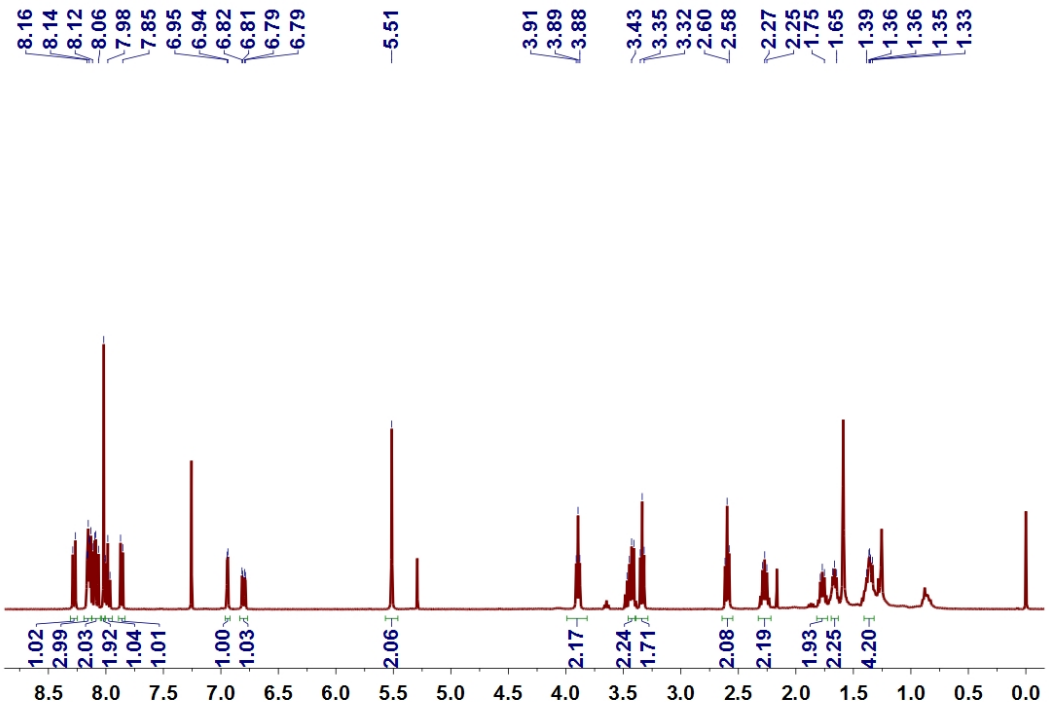

Fig. S4. ^{1}H NMR spectrum (400 MHz, chloroform-*d*, 293 K) of **3**.

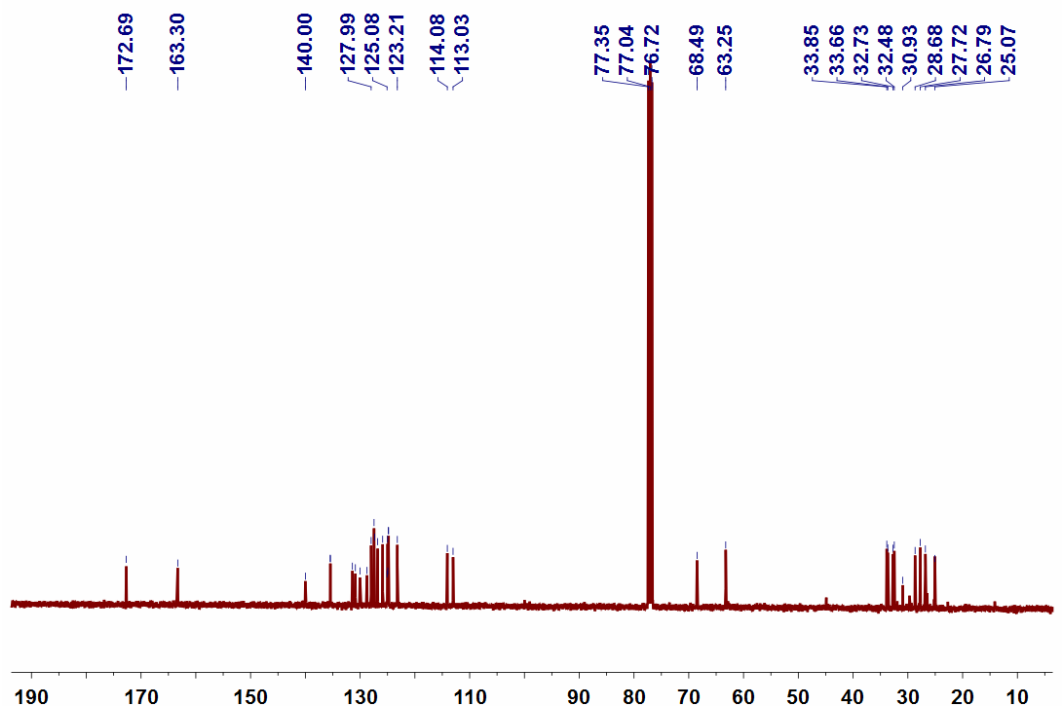

Fig. S5. ^{13}C NMR spectrum (100 MHz, chloroform-*d*, 293 K) of **3**.

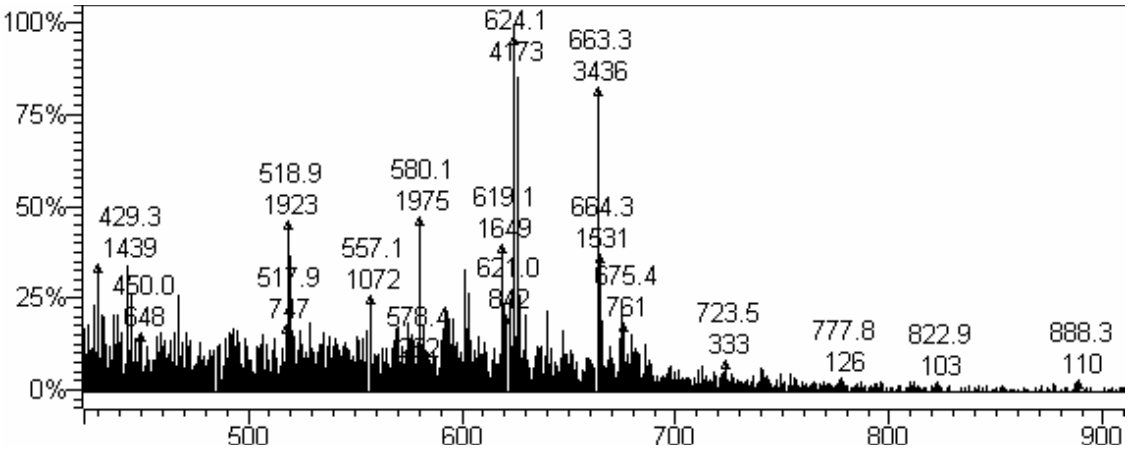

Fig. S6. Electrospray ionization mass spectrum of **3**. Assignment of the main peak: *m*/*z* 624.1 $[M + Na]^+$ (100%).

Synthesis of **G**: Compound **3** (1.00 g, 1.66 mmol) and 3,5-dimethylpyridine (1.78 g, 16.6 mmol) were added to 100 mL acetonitrile and refluxed over night. After reaction, solvents and excess 3,5-dimethylpyridine were removed by rotary evaporation to gain **G** as yellow powder (1.01 g, 90%), m.p. 123.0–124.2 ºC. The ^{1}H NMR spectrum of **G** is shown in Fig. S7. ^{1}H NMR (400 MHz, DMSO, 293 K) δ (ppm): 8.78 (s, 2H), 8.37 (d, J = 8 Hz, 1H), 8.26 (d, J = 8 Hz, 3H), 8.22 (d, J = 8 Hz, 1H), 8.18 (d, J = 4 Hz, 2H), 8.12 (s, 2H), 8.05 (t, J = 8 Hz, 1H), 7.95 (d, J = 8 Hz, 1H), 7.09 (s, 2H), 5.43 (s, 2H), 4.40 (t, J = 8 Hz, 2H), 4.04 (t, J = 8 Hz, 2H), 2.63 (t, J = 8 Hz, 2H), 2.41 (s, 6H), 2.10 (t, J = 8 Hz, 2H), 1.80 (d, J = 8 Hz, 2H), 1.34 (s, 2H). The ^{13}C NMR spectrum of **G** is shown in Fig. S8. ^{13}C NMR (100 MHz, DMSO, 293 K) δ (ppm): 172.35, 162.80, 146.03, 141.40, 139.78, 137.82, 136.01, 134.83, 130.81, 130.32, 129.33, 127.96, 127.46, 127.36, 127.26, 126.54, 126.12, 124.90, 124.79, 124.16, 124.31, 123.32, 114.60, 113.66, 68.32, 62.67, 60.27, 33.16, 31.88, 30.35, 27.95, 26.74, 25.00, 24.66 and 17.65. LRESIMS is shown in Fig. S9: *m*/*z* 629.6 $[M + NH_4]^+$. HRESIMS: *m*/*z* calcd for $[M + NH_4]^+$ $C_{40}H_{41}N_2O_5$, 629.3015; found 629.3033; error 3 ppm.

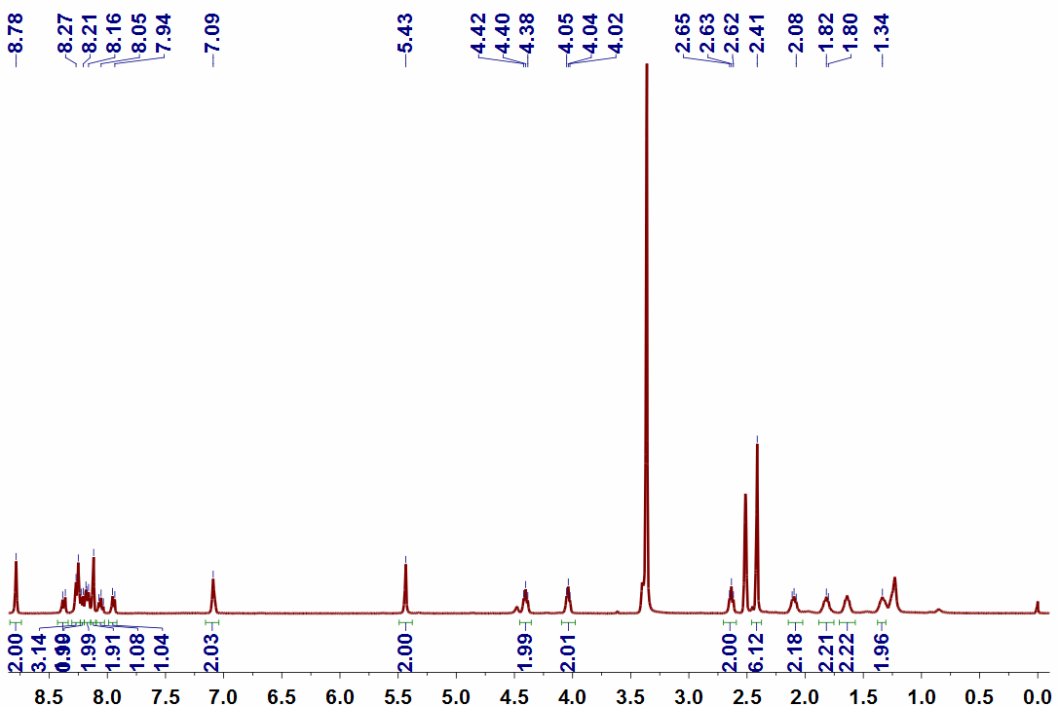

Fig. S7. ^{1}H NMR spectrum (400 MHz, DMSO-d_6, 293 K) of **G**.

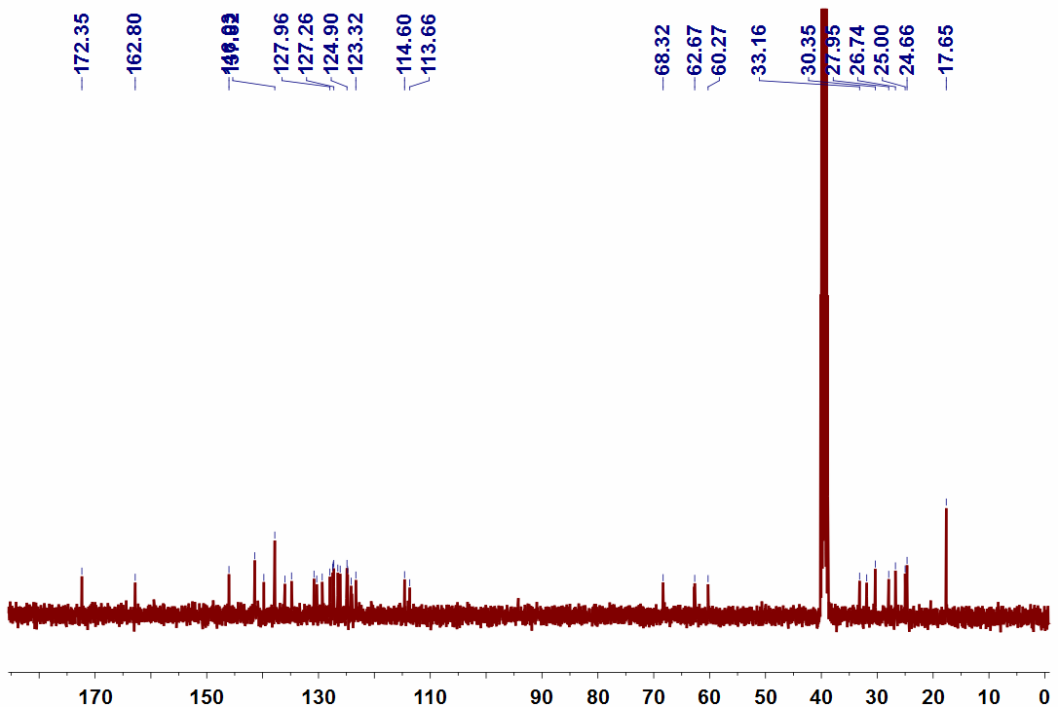

Fig. S8. ^{13}C NMR spectrum (100 MHz, DMSO-d_6, 293 K) of **G**.

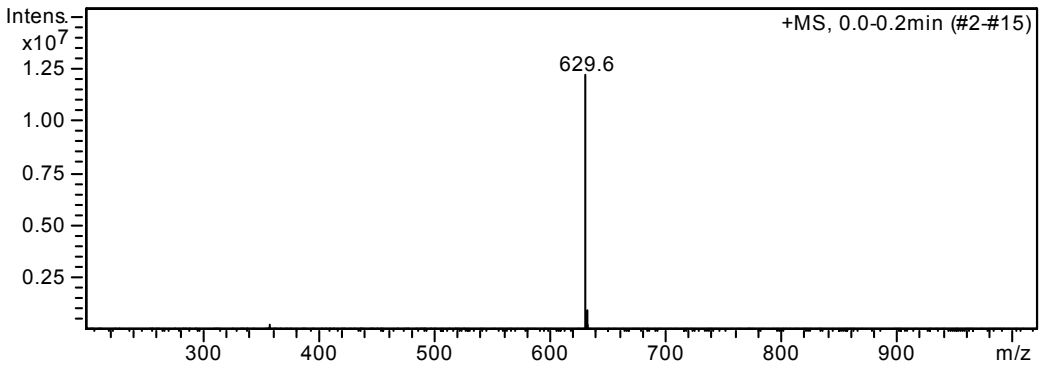

Fig. S9. Electrospray ionization mass spectrum of **G**. Assignment of the main peak: *m*/*z* 629.6 $[M + NH_4]^+$ (100%).

Scheme S2. Synthetic route to **DMPy**.

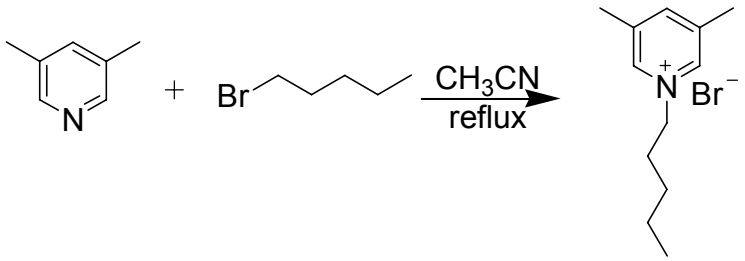

DMPy

Synthesis of **DMPy**: 3,5-Dimethylpyridine (2.14 g, 20.0 mmol) and excessive 1-bromopentane were added to 100 mL of acetonitrile and refluxed over night. After reaction, the solvent was removed by rotary evaporation and the resultant residue was washed thrice with CH_2Cl_2 to remove the excess 1-bromopentane. After drying, **DMPy** was obtained as a brown liquid (4.86 g, 94%). The ^{1}H NMR spectrum of **DMPy** is shown in Fig. S10. ^{1}H NMR (400 MHz, D_2O, 293 K) δ (ppm): 8.39 (s, 2H), 8.07 (s, 1H), 4.39 (t, J = 8 Hz, 2H), 2.38 (s, 6H), 1.87 (m, 2H), 1.20 (m, 4H), 0.75 (t, J = 8 Hz, 3H). The ^{13}C NMR spectrum of **DMPy** is shown in Fig. S11. ^{13}C NMR (100 MHz, D_2O, 293 K) δ (ppm): 146.38, 140.85, 138.92, 30.17, 27.36, 17.41, and 13.03. LRESIMS is shown in Fig. S12: *m*/*z* 178.1 $[M - Br]^+$. HRESIMS: *m*/*z* calcd for $[M - Br]^+$ $C_{12}H_{20}N$, 178.1596; found 178.1601; error 3 ppm.

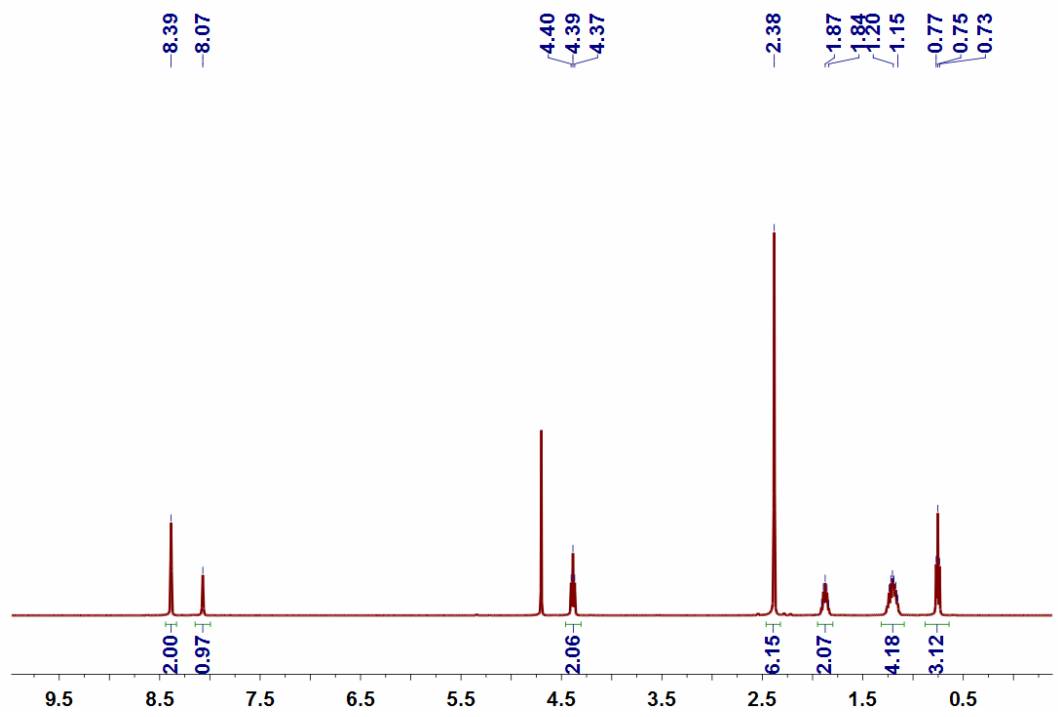

Fig. S10. ^{1}H NMR spectrum (400 MHz, D_2O, 293K) of **DMPy**.

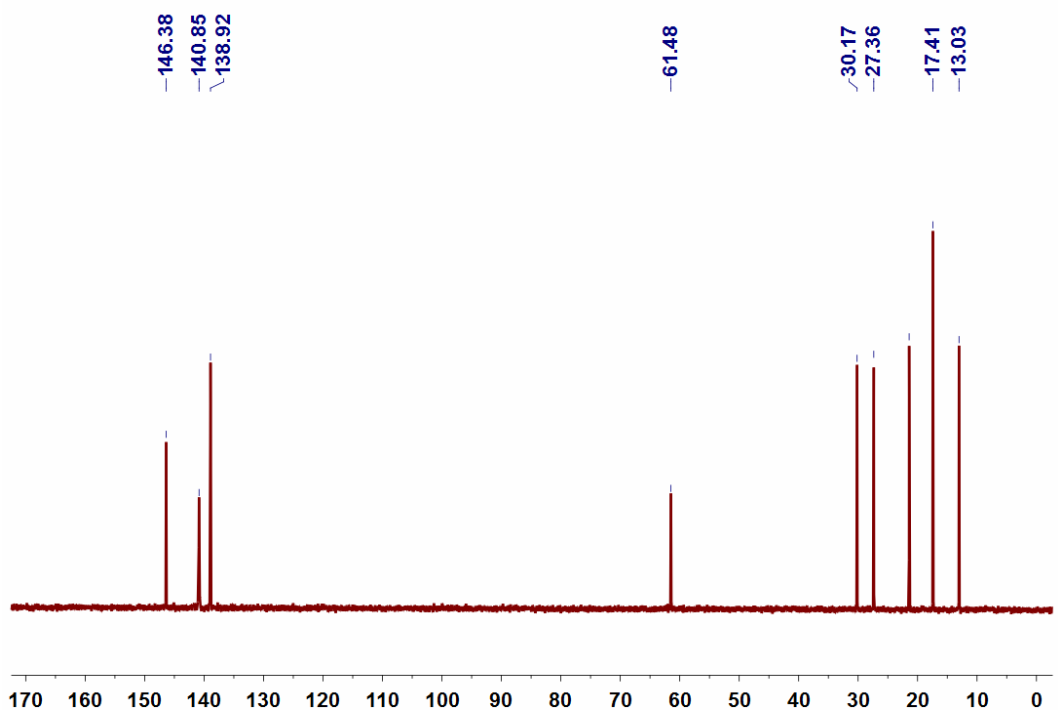

Fig. S11. ^{13}C NMR spectrum (100 MHz, D_2O, 293K) of **DMPy**.

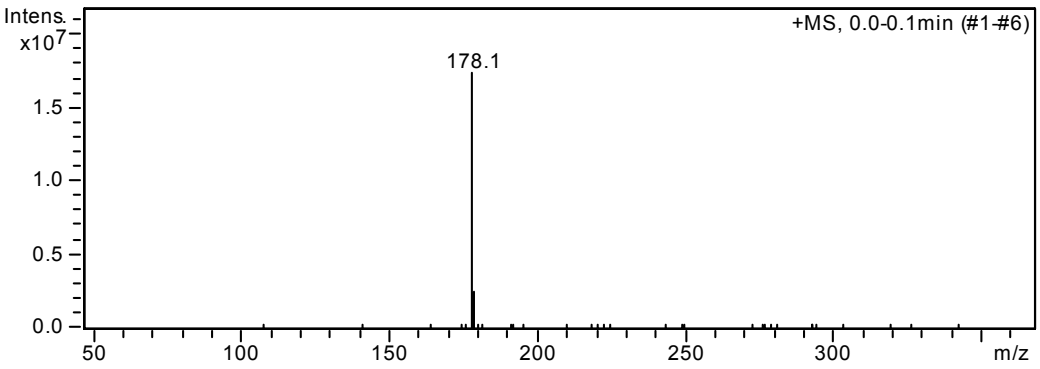

Fig. S12. Electrospray ionization mass spectrum of **DMPy**. Assignment of the main peak: *m*/*z* 178.1 $[M - Br]^+$ (100%).

*3. Investigation of the complexation between model compound **DMPy** and **WP6***

To determine the stoichiometry and association constant for the complexation between host **WP6** and guest **DMPy**, fluorescence titration experiments were done with solutions which had a constant concentration of **WP6** (5.00×10^{-6} M) and varying concentrations of the guest. By a non-linear curve-fitting method, the association constant (K_a) of **WP6⊃DMPy** was estimated. By mole ratio plot, 1:1 stoichiometry was obtained for the complexation between **WP6** and **DMPy**.

The non-linear curve-fittings were based on the equation:

$$\Delta F = (\Delta F_\infty/[H]_0)\ (0.5[G]_0 + 0.5([H]_0+1/K_a) - (0.5\ ([G]_0^2+(2[G]_0(1/K_a - [H]_0)) + (1/K_a + [H]_0)^2)^{0.5}))$$

Where ΔF is the fluorescence intensity changes at 326 nm at $[G]_0$, ΔF_∞ is the fluorescence intensity changes at 326 nm when **WP6** is completely complexed, $[G]_0$ is the initial concentration of **G**, and $[H]_0$ is the fixed initial concentration of **WP6**.

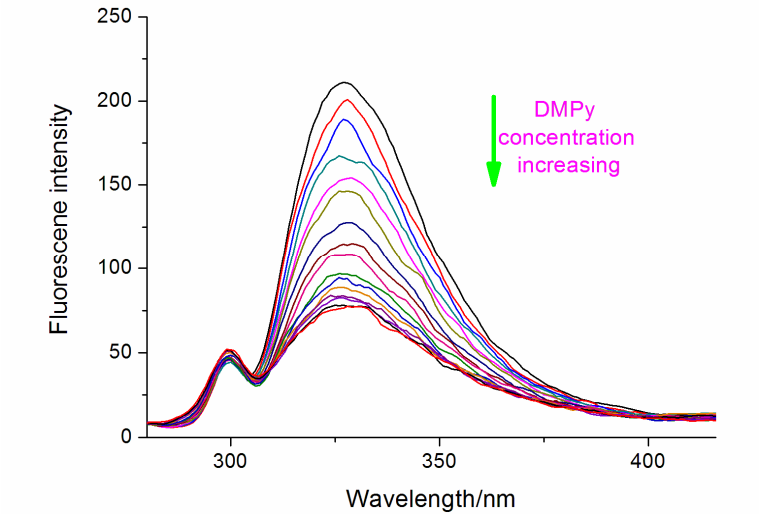

Fig. S13. Fluorescence spectra of **WP6** (5.00×10^{-6} M) upon addition of **DMPy** gradually in water at room temperature.

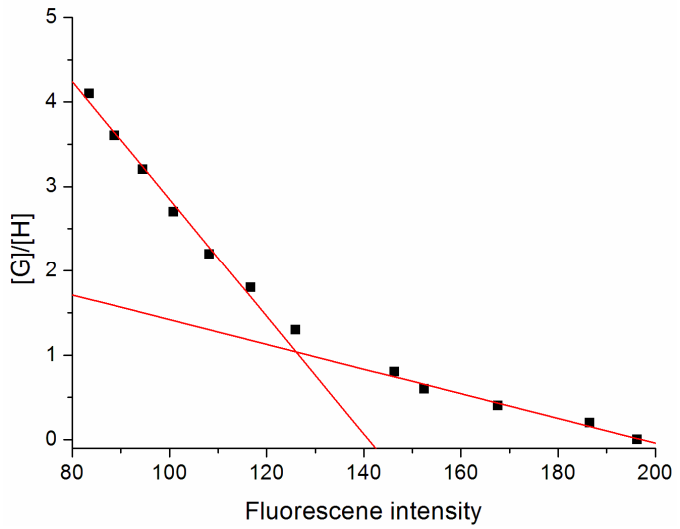

Fig. S14. Mole ratio plot for **WP6** and **DMPy**, showing a 1:1 complexation stoichiometry.

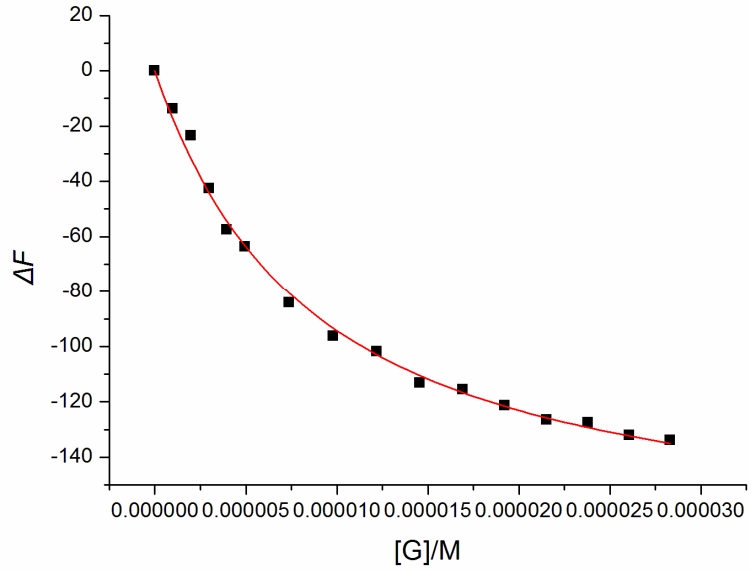

Fig. S15. The fluorescence intensity changes of **WP6** upon addition of **DMPy**. The red solid line was obtained from the non-linear curve-fitting method based on the above equation.

*4. UV-vis spectroscopy data of the complexation between **WP6** and **DMPy** in H_2O*

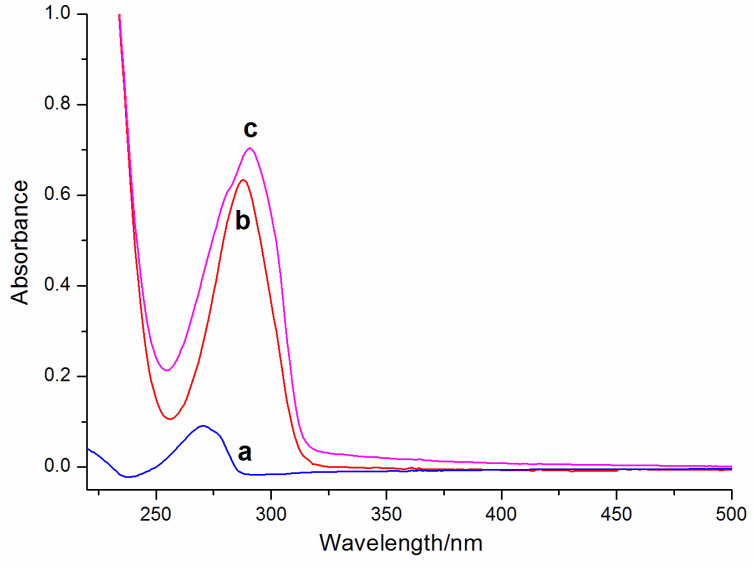

Fig. S16. UV-vis spectra of (a) **WP6**, (b) **DMPy**, and (c) **DMPy** in the presence of 1 equiv of **WP6** (2.50×10^{-5} M) in water.

*5. ^1H NMR spectra of **WP6⊃DMPy***

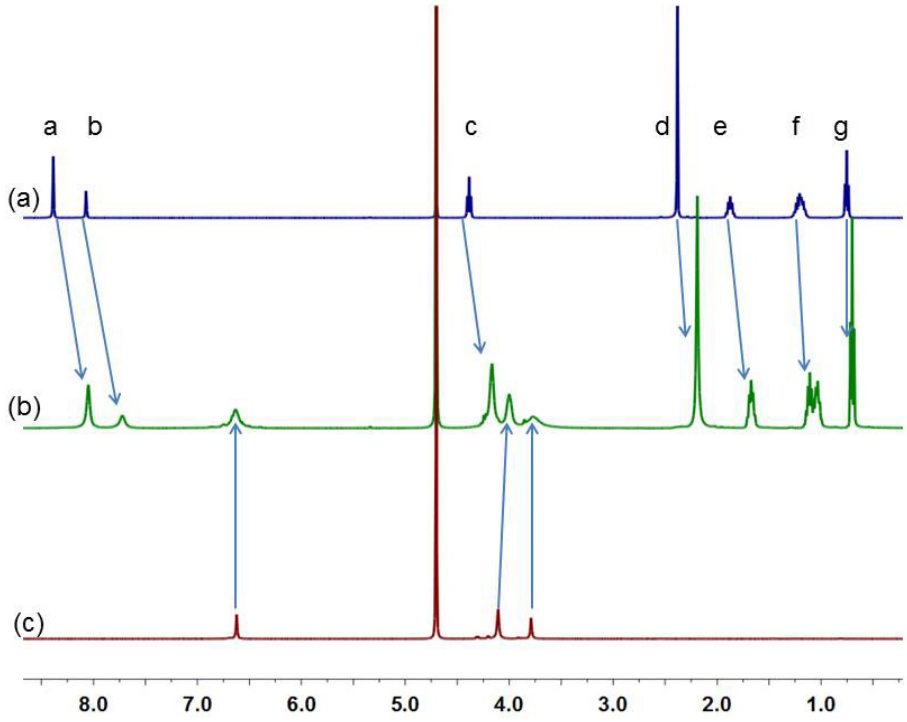

Fig. S17. Partial ^{1}H NMR spectra (500 MHz, D_2O, room temperature): (a) **DMPy** (1.00 mM); (b) **DMPy** (1.00 mM) and **WP6** (1.00 mM); (c) **WP6** (1.00 mM)

*6. Critical aggregation concentration (CAC) determination of **G** and **WP6⊃G***

Some parameters such as the conductivity, osmotic pressure, fluorescence intensity and surface tension of the solution change sharply around the critical aggregation concentration. The dependence of the solution conductivity on the solution concentration is used to determine the critical aggregation concentration. Typically, the slope of the change in conductivity versus the concentration below CAC is steeper than the slope above the CAC. Therefore, the junction of the conductivity-concentration plot represents the CAC value. To measure the CAC value of **G** (or **WP6⊃G**), the conductivities of the solutions at different concentrations were determined. By plotting the conductivity versus the concentration, we estimated the CAC value of **G** (or **WP6⊃G**).

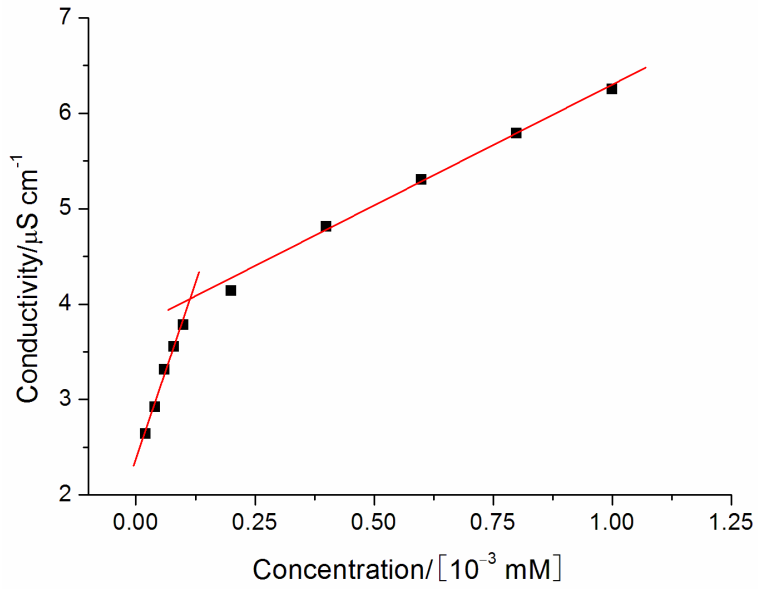

Fig. S18. The concentration-dependent conductivity of **G**. The critical aggregation concentration (CAC) was determined to be 1.1×10^{-7} M.

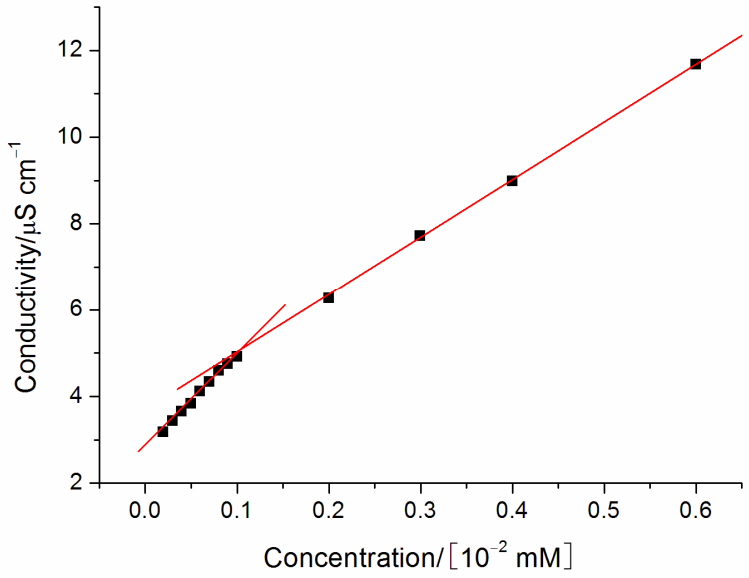

Fig. S19. The concentration-dependent conductivity of **WP6⊃G**. The aqueous solutions used here are equivmolar solutions of **WP6** and **G** in water. The critical aggregation concentration (CAC) was determined to be 1.0×10^{-6} M.

7. TEM image of pyrene-1-butyric acid.

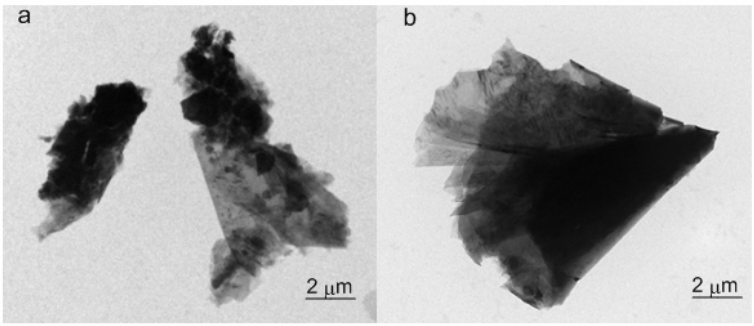

Fig. S20. TEM images: (a) **WP6⊃G** treated with UV light irradiation; (b) pyrene-1-butyric acid.

*8. Further evidence for the formation of **WP6⊃G.***

In order to confirm the threading of **G** through the cavity of **WP6**, another model compound **OPB** was synthesized according to a procedure described in the literature.[S2] The host–guest complexation between **WP6** and **OPB** was studied by ^{1}H NMR spectroscopy and 2D ^{1}H-^{1}H NOESY spectroscopy. As shown in Fig. S21, significant chemical shift changes corresponding to the protons of **OPB** were observed in the presence of **WP6**. The signals of **OPB** all shifted upfield and became broaden. On the other hand, the protons on **WP6** also exhibited slight changes due to the interactions between **OPB** and **WP6**, indicating the formation of a threaded structure between **OPB** and **WP6**. As shown in Fig. S22, correlation signals were observed between protons $H_{a\text{-}e}$ on **OPB** and protons H_{1-3} on **WP6**, indicating that **OPB** penetrated into the cavity of **WP6**.

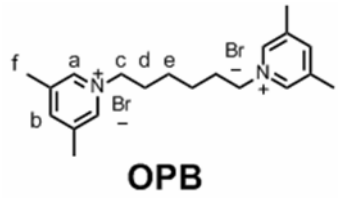

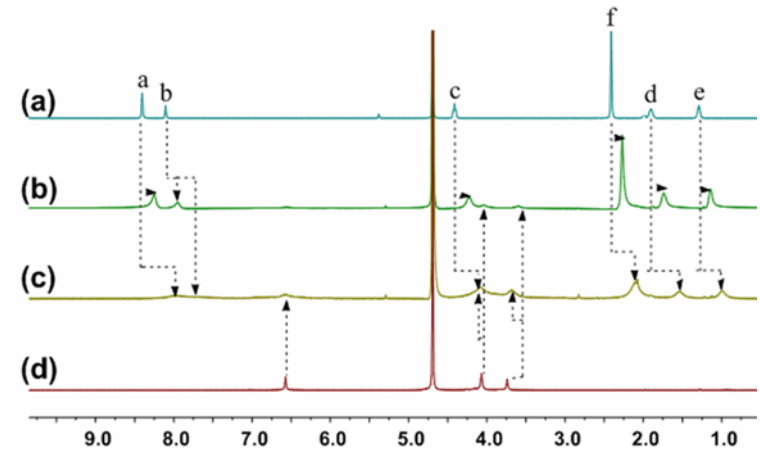

Fig. S21. Partial ^{1}H NMR spectra (500 MHz, D_2O, room temperature): (a) **OPB** (1.00 mM); (b) **OPB** (3.00 mM) and **WP6** (1.00 mM); (c) **OPB** (1.00 mM) and **WP6** (1.00 mM); (d) **WP6** (1.00 mM).

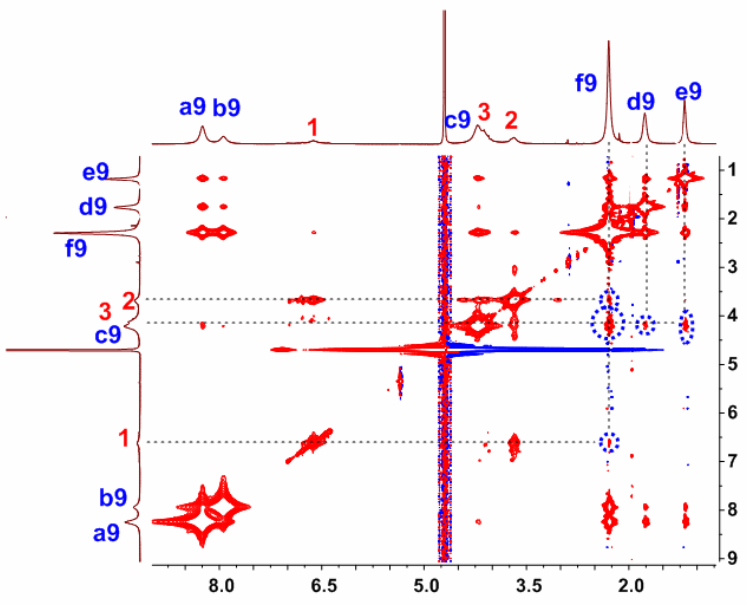

Fig. S22. 2D ^{1}H-^{1}H NOESY spectrum of **WP6⊃OPB** (500 MHz, D_2O, room temperature).

*9. Determination of the association constant between **WP6** and **DMPy** in water.*

By using the Stern–Volmer equation, the association constant between **WP6** and **DMPy** was calculated to be $(1.87 \pm 0.09) \times 10^5$ M^{-1}, in consistent with the results obtained from the above fluorescence titration experiments.

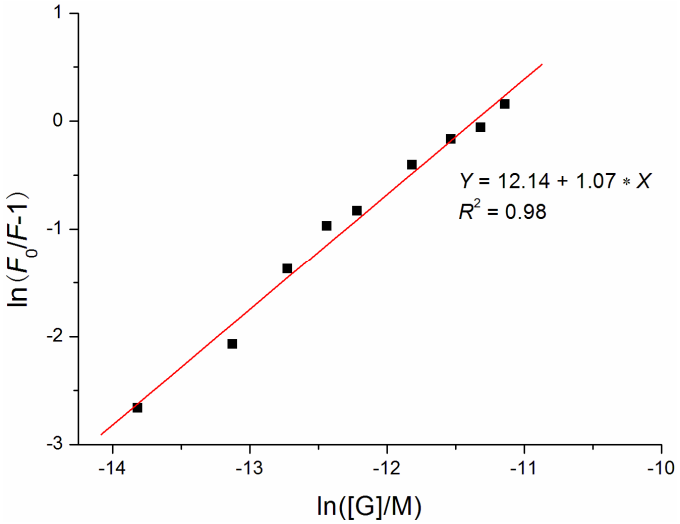

Fig. S23. The plot of the Stern-Volmer equation ln $(F_0/F - 1)$ = ln K + n ln ([G]/M) for the complexation using the fluorimetric titration data at λ = 326 nm. F_0 is the initial fluorescent emission intensity of **WP6** and F is the fluorescent emission intensity of **WP6** in the presence of different concentrations of **DMPy**.

10. TEM image of the intermediate state from nanosheets to nanospheres.

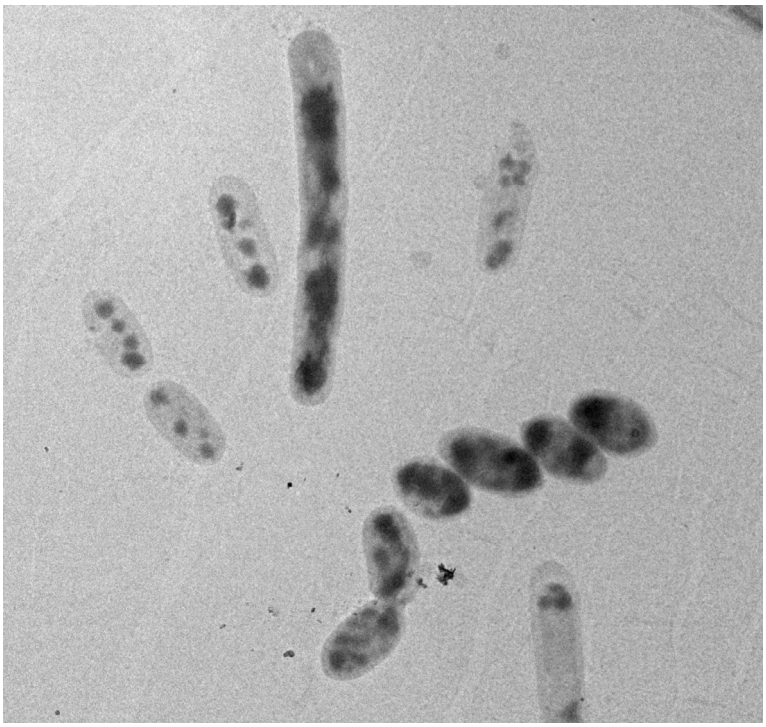

Fig. S24. TEM image of the intermediate state from nanosheets to nanospheres**.**

*11. Photograph of an aqueous solution of **WP6⊃G**/MWNTs.*

WP6⊃G/MWNTs hybrids were prepared by sonication of **WP6⊃G** (40.0 mg, 1:1 in molar ratio) in water (10 mL) with 1.00 mg MWNTs. During the sonication, the color of the aqueous solution changed from colorless to black. After the sonication, insoluble MWNTs were removed by centrifugation. The supernatant was dialyzed against water for 2 weeks to remove excess free **WP6⊃G** from the solution. Another sample of the original untreated MWNTs was also studied as a control experiment. The black solution of the **WP6⊃G**/MWNTs complex was homogeneous and stable and could stand for >1 month without significant change.

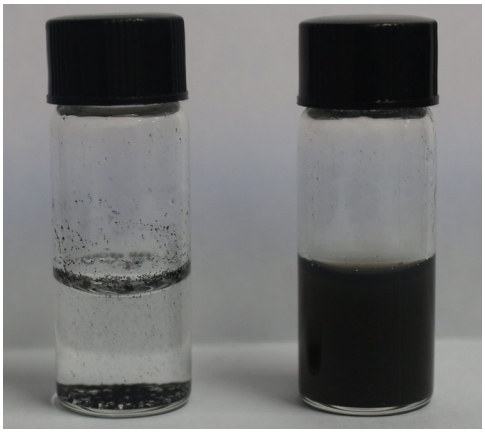

Fig. S25. Photograph: (left) original untreated MWNTs in water; (right) **WP6⊃G/**MWNTs in water.

References:

S1. (a) J. Yin, H. Hu, Y. Wu and S. Liu, *Polym. Chem.*, 2011, **2**, 363–371; (b) G. Yu, M. Xue, Z. Zhang, J. Li, C. Han and F. Huang, *J. Am. Chem. Soc.*, 2012, **134**, 13248−13251.

S2. C. Li, X. Shu, J. Li, S. Chen, K. Han, M. Xu, B. Hu, Y. Yu and X. Jia, *J. Org. Chem.,* 2011, **76**, 8458–8465.